8.2 GLOBALLY DESCRIBING THE CURRENT DAY LAND SURFACE AND HISTORICAL LAND COVER CHANGE IN CCSM 3.0 USING AVHRR AND MODIS DATA AT FINE SCALES

Peter J. Lawrence *
Cooperative Institute for Research in Environmental Sciences (CIRES),
University of Colorado, Boulder

1. INTRODUCTION

Tian et al., (2004a)*, Oleson et al.*, (2003), and *Tian et al.*, (2004b) recently identified significant differences between the current land surface parameters of the Community Land Model (CLM) used with the Community Climate System Model (CCSM), and global land surface descriptions from Moderate Resolution Imaging Spectroradiometer (MODIS) satellite mapping. Specifically these investigations identified significant differences in Leaf Area Index (LAI), Fraction of Photosynthetically Active Radiation (FPAR), and land surface albedo. *Tian et al.*, (2004a) suggested that these differences in land surface representation, especially land surface albedo, may significantly affect the accuracy of climate simulation of the CCSM model.

To asses whether these differences in land surface representation do have significant impacts on the climate modeled in the CLM and the CCSM, new land surface parameters have been developed from land surface data derived from NOAA Pathfinder Advanced Very High Resolution Radiometer (AVHRR) and MODIS satellite data that minimise these differences. The impact on the climate simulated in the CCSM with these new parameters was assessed through a climate sensitivity experiment with the new parameters against a control experiment with the current land surface parameters. The climate modeled in these sensitivity experiments were compared with globally observed climate data to evaluate the climate impacts that the new land surface parameters had at global, continental and regional scales.

2. THE NCAR COMMUNITY CLIMATE SYSTEM MODEL

The newest version of the NCAR Community Climate System Model (CCSM 3.0) includes a new standard land surface parameterization, the Common Land Model (CLM 3.0), representing an improvement over previous land surface representations in the CCM family of models. The CLM simulates the land surface more realistically both in the description of physical processes and in the use of more representative land surface boundary data. Both of these changes helped to improve the overall climate simulation *Zeng et al.*, (2002).

Capturing the dynamics and spatial heterogeneity of MODIS land surface data in climate models is a complex process, as the physical phenomena observed by the satellite and compiled through data processing, must be represented through the land surface parameters of the climate model. The CLM land surface model allows sub-grid heterogeneity to be described through fractional allocation of land cover to four functional plant types (PFTs) as well as describing the percentage of each grid cell occupied by ocean, lakes, wetlands, and glaciers. The properties of each of the sub-grid land fractions are described through both monthly varying grid cell specific PFT parameters, as well as time and space invariant PFT and soil column parameters.

The goal in generating new land surface parameters was to develop parameters that when used in the CLM model would reproduce the land surface conditions captured in the AVHRR and MODIS satellite data as closely as possible. To ensure that the new land surface parameters could be used over a range of model resolutions and in finer scale land cover change experiments, the new model parameters were developed at the relatively fine-scale resolution of 0.05 degrees, which can then be aggregated to the fractional land cover parameters of the CLM at a required grid interval.

3. NEW PLANT FUNCTIONAL TYPE MAPPING

The mapping of CLM PFT distributions was performed following the original methods used for

* *Corresponding author address:* Peter J. Lawrence, Cooperative Institute for Research in Environmental Sciences (CIRES), University of Colorado, Boulder, 80309, USA
email: peterjohn.lawrence@colorado.edu

PFT parameters in CLM 2.0 by *Bonan et al.*, (2002), with the physiology and climate rules developed by *Nemani and Running*, (1996). As in the original mapping, the percentage Tree Cover, Leaf Type, and Leaf Longevity were derived from AVHRR Continuous Fields Tree Cover Project data from *Defries et al.*, (2000). To address the over prescription of understorey PFTs, in particular grass, identified by *Tian et al.*, (2004a), the 0 – 80% cover values of the raw tree cover data were scaled to 0 – 100% PFT values for the PFT mapping.

Understorey and herbaceous PFT distributions were derived from IGBP Global Land Cover Characterization land cover mapping, with the distribution of C3/C4 grass mapped following the fractional C3/C4 mapping methods of *Still et al.*, (2003). Climate data used for the PFT climate rules was compiled from 1970 – 1999 monthly surface air temperature and precipitation surfaces generated by *Willmott and Matsuura*, (2000) from the Global Historical Climate Network.

The 0.05 degree PFT maps were aggregated to the T42 grid increment of the CCSM model to generate the new CLM land surface parameters. Where more than four PFTs existed within a grid cell the smallest PFT fraction was grouped with similar PFTs in a hierarchical grouping scheme. The main differences between the PFT distributions were for an increase in tree PFTs at the expense of understorey PFTs with the new methods. There also are significant differences in the distribution of C3 and C4 grasses. The new methods better separated C4 grasses to warmer, wetter tropical areas, and confined C3 grasses to cooler latitudes and altitudes.

4. NEW LEAF AREA INDEX (LAI) AND STEM AREA INDEX (SAI) MAPPING

To address differences in monthly LAI and SAI, new CLM parameters were derived from quality assured and averaged MODIS V4 LAI data *Myneni et al.*, (1997). The LAI data was averaged from the 2001 – 2003 monthly values at the 0.05 degree resolution. The grid averaged monthly LAI values were used to calculate monthly PFT LAI values for each 0.05 degree grid cell based on the PFT percentage values and the relative PFT LAI max values of each PFT within a grid cell. The significant improvement with the new LAI methods was consistency with MODIS LAI when the PFT LAIs were combined with the PFT percentages to reproduce average monthly LAI values for the vegetated fraction of each model grid cell.

The new methods also used additional rules to enforce seasonal leaf phenology, and to calculate monthly PFT SAI values from minimum PFT SAI values and the calculated monthly PFT LAI values. The new methods enforced the leaf phenology of Summer Green Deciduous Trees through Growing Degree Days (GDD) from a base growing temperature (TBase) following the LPJ dynamic vegetation model of *Sitch et al.*, (2003). Evergreen leaf phenology and SAI were calculated using the methods of *Zeng et al.*, (2002), with the grid cell average minimum PFT SAI values (Lsmin) calculated from individual plant values provided by *Zeng et al.*, (2002). The scaling of plant minimum PFT SAI values to grid values was based on the ratio of the maximum monthly grid cell PFT LAI values to the individual plant maximum PFT LAI values from *Bonan et al.*, (2002). The aggregation of the 0.05 degree PFT values to the model grid interval included averaging of LAI, SAI and height parameters based on PFT percentages and PFT groupings.

The differences in combined PFT LAI and SAI values of the new methods and the current CLM parameters are shown in *figure 1*. The new methods LAI values closely reflect the original monthly MODIS values, and have large differences with the current parameters for both Austral summer (DJF) and Boreal summer (JJA). The largest DJF differences occur in southern South America, Africa and Australia, where the MODIS derived values are significantly lower than the current CLM parameters. There also are large year round differences in Amazonian, central African and South East Asian tropical forests, where the MODIS derived values are significantly higher than the current parameters. In JJA, the MODIS derived values are consistently lower over most of North America, Europe and coastal Australia.

There are also large differences in both DJF and JJA for SAI, with the new parameters having significantly lower SAI values in sparsely vegetated areas of the Southern Hemisphere in DJF and the Northern Hemisphere in JJA. There also are year round differences in tropical forests with the new parameters having higher SAI values for both DJF and JJA.

.

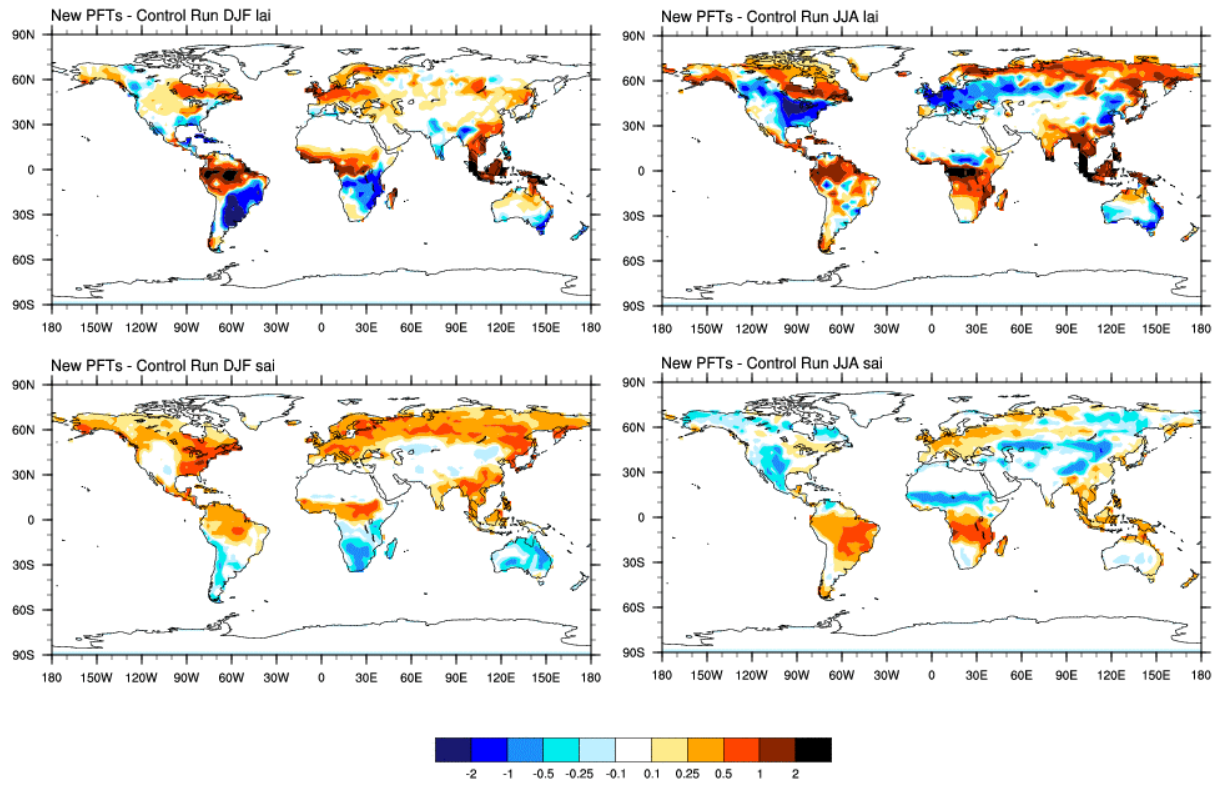

FIG. 1 Differences in CLM Leaf Area Index (LAI) and Stem Area Index (SAI) at the T42 grid increment for New Parameters and Control (CLM) Parameters.

5. NEW LEAF AND STEM RADIATION PARAMETERS AND SOIL REFLECTANCE MAPPING

In order to address albedo differences between the two stream radiation model of the CLM and MODIS, new monthly leaf and stem radiation properties, as well as soil reflection maps were derived from MODIS Version 4 albedo data (*Schaaf et al.*, 2002). The methods used average monthly snow and cloud corrected Black Sky (Direct Beam) and White Sky (Diffuse Beam) albedo values for each spectrum to calculate the values for leaf, stem and soil reflectance that would reproduce the MODIS values when used in the two stream model.

In order to separate the contributions of canopy and soil reflectance and absorption, the two stream radiation model was used to fit mean leaf and stem optical properties for each PFT in canopies where soil reflectance contributed less than 5 percent to the radiation dynamics. Once leaf and stem properties were calculated soil reflectance values were fitted to the model using the new PFT values, PFT fractions, and monthly PFT LAI and SAI values.

The new methods produced lower values for visible reflectance and transmittance for most, with the exception of Evergreen and Temperate Shrubs which were higher. There were mixed changes for near infrared reflectance and transmittance with the new methods. Most tree PFTs had higher values, while shrubs and grasses were mostly unchanged. The exception in the near infrared was PFTs was Broadleaf Evergreen Temperate trees which had lower reflectance and transmittance values. The exceptionally high stem transmittance values of grasses also were returned to the same value as other PFTs. The new visible and near infrared soil reflectance distributions strongly reflect MODIS values, with sparsely vegetated areas having significantly higher reflectance than densely vegetated areas for both seasons and spectral bands.

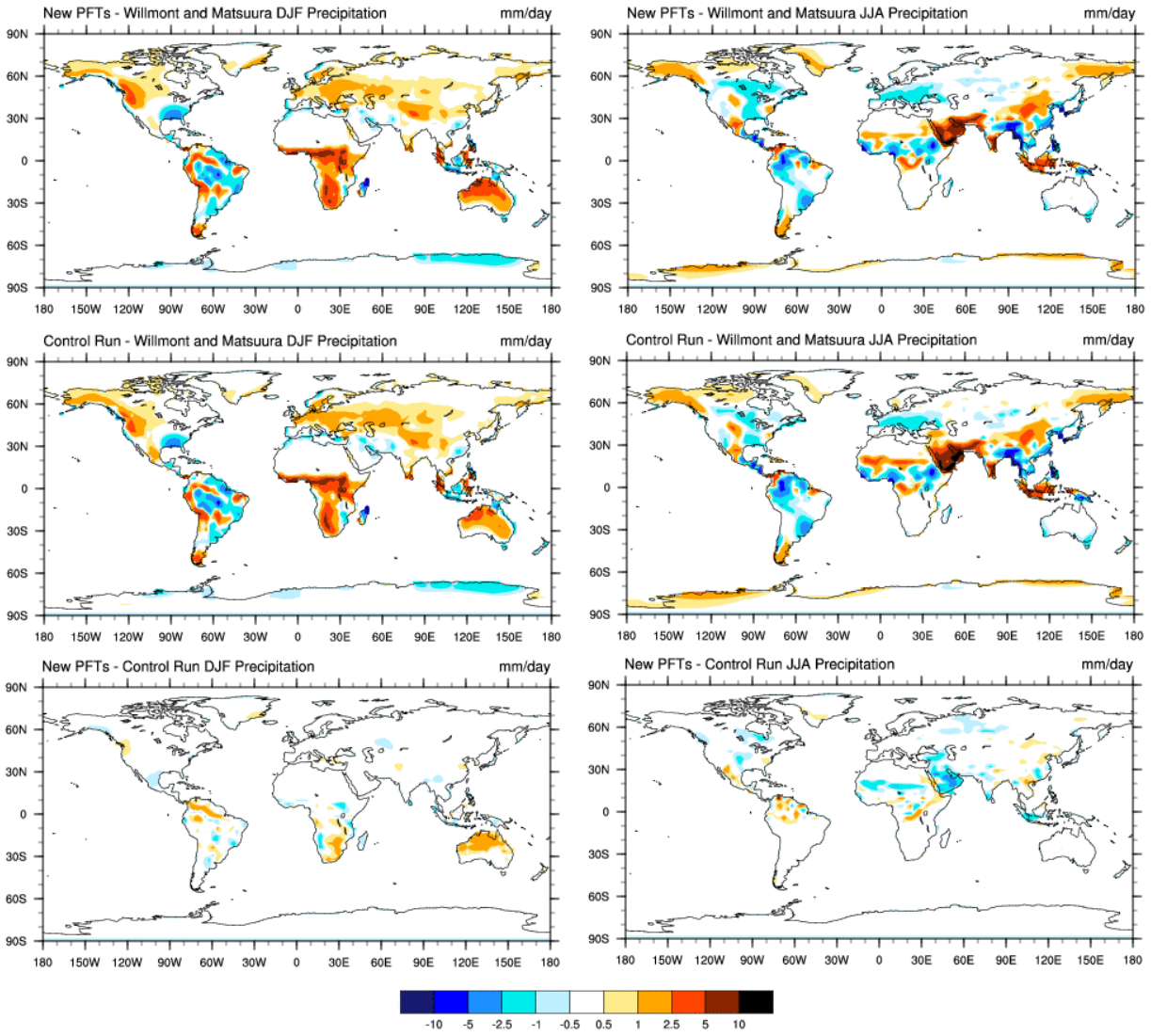

FIG. 2 Seasonal distributions and differences between Observed and modeled CCSM Precipitation at the T42 grid increment for New Parameters Experiment and Control Experiment

6. NEW LAND SURFACE PARAMETER SENSITIVITY EXPERIMENTS

To investigate the climate impacts of the new methods on the CLM and CCSM models, a sensitivity experiment was performed with the new land surface parameters compared to a control experiment with the current parameters. The experiments were performed at the T42 grid interval using prescribed monthly climatology sea surface temperatures and sea ice distributions. The experiments were each run for a 15 year period, with the initial 5 years discarded as a spin up period.

The differences between the experiments were assessed relative to model biases from other sources, by comparing model results to observed climatology data from *Willmott and Matsuura*, (2000) for precipitation and 2 meter air temperature, and from MODIS for snow cover extent and surface albedo. The average monthly precipitation and air temperature data were compiled from 1970 – 1999 monthly values, aggregated from the 0.5 degree resolution to the T42 grid increment. The monthly MODIS snow

cover and surface albedo were compiled from 2001 – 2003 Version 4 fortnightly albedo data, with snow cover derived from the snow cover percentage of the quality assurance product. The 0.05 degree MODIS data was aggregated to the T42 grid increment using a land mask to remove some of the water biases identified in *Oleson et al.*, (2003).

7. RESULTS

The differences in precipitation between the experiments and observed values (*figure 2*) showed there were consistent patterns of climate bias in the CCSM model with both sets of parameters. In DJF the consistently high bias over central and southern Africa was not significantly changed with the new parameters, however the high bias in monsoon in Australia was increased. In JJA the consistently high precipitation biases over the Sahel, and from the Saudi peninsula to Pakistan were significantly reduced with the higher albedo over the Sahara and Saudi peninsula in the new parameters.

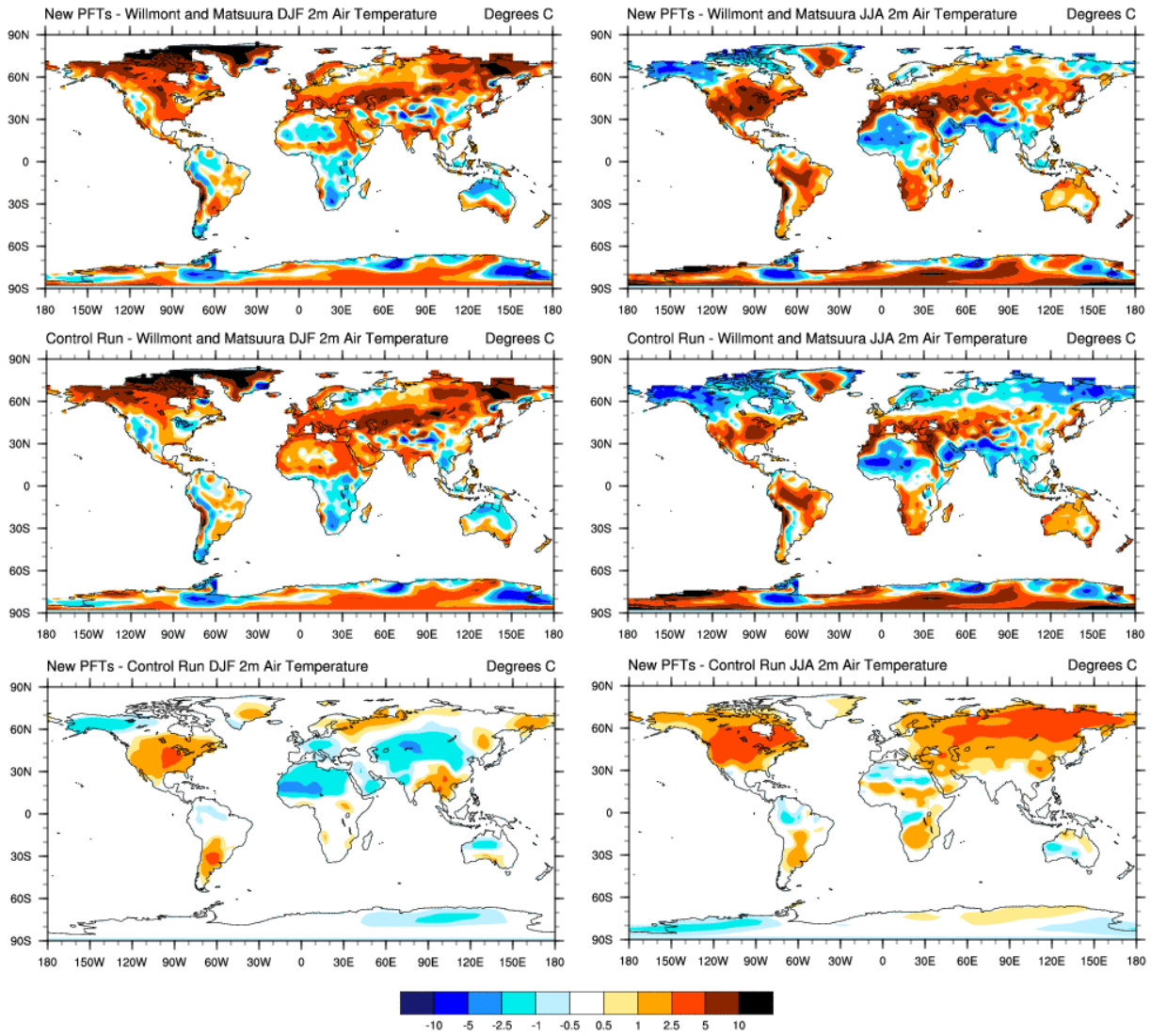

FIG. 3 Seasonal distributions and differences between Observed and modeled CCSM Air Temperature at 2 meters at the T42 grid increment for New Parameters Experiment and Control Experiment

.

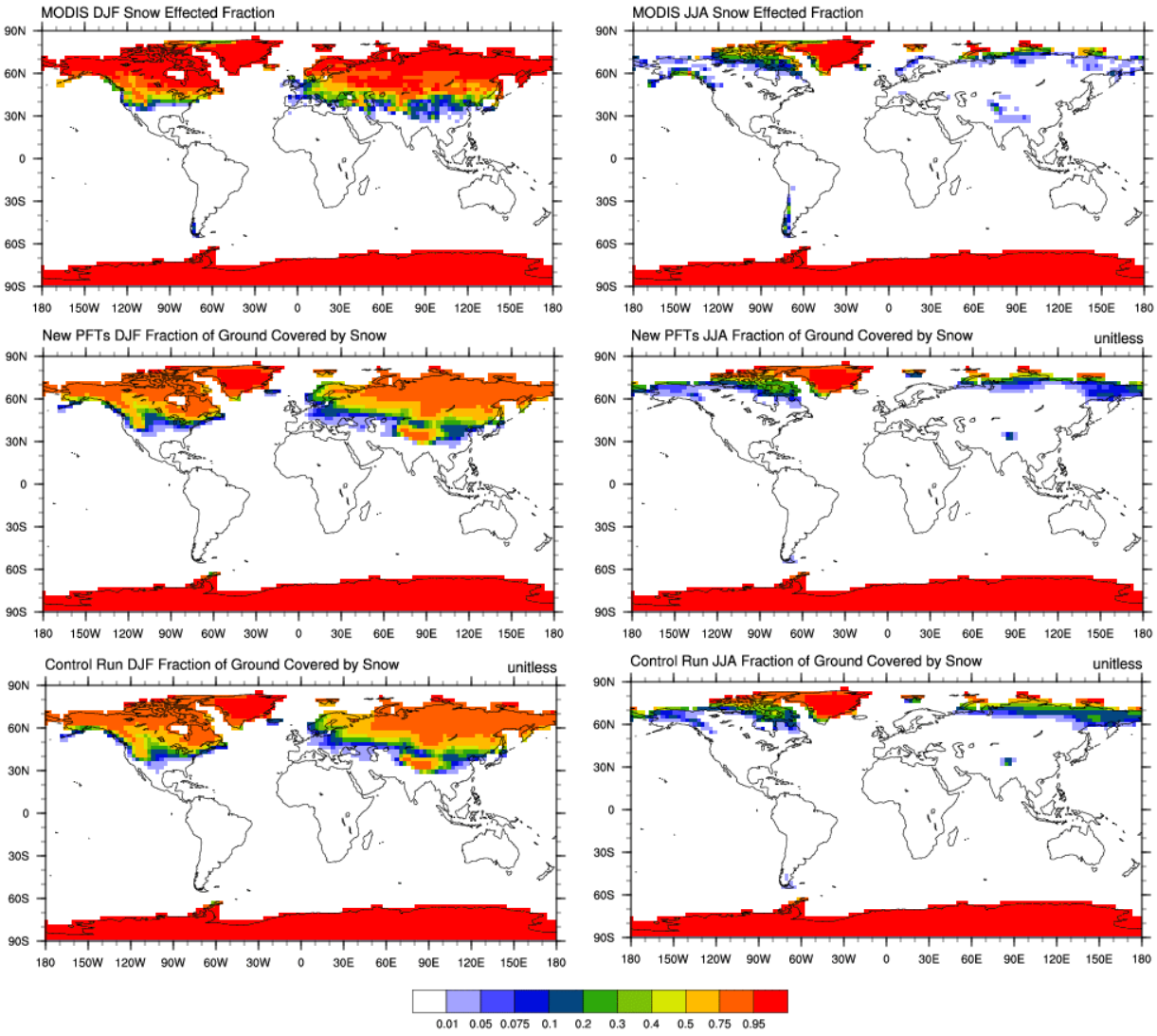

FIG. 4 Seasonal distributions and differences between MODIS and CCSM Fractional Snow Cover at the T42 grid increment for New Parameters Experiment and Control Run Experiment

The differences in 2 meter air temperature between the experiments and observed values (*figure 3*) also showed there were similar patterns of climate bias in the CCSM model with both sets of parameters. However, these differences were not as consistent as the precipitation, with the differences between the experiments showing the impacts of the new parameters. In DJF the warm bias over the Sahara, the Saudi peninsula, and Eurasia were all reduced with the new parameters, however, the warm bias over North America was increased. In JJA the cold bias over northern Russia and Siberia were reduced or removed, the warm bias over North America was increased, and the cool bias over the Sahel reduced.

The new parameters were highly effective in reducing the surface albedo differences between MODIS and the two stream radiation model in snow free areas (*figure 5*). In snow affected areas however, there were very large differences in surface albedo. As the albedo differences due to soil and vegetation differences had been effectively removed with the new parameters, these remaining albedo differences supported the albedo snow impacts suggested by *Oleson et al.*, (2003).

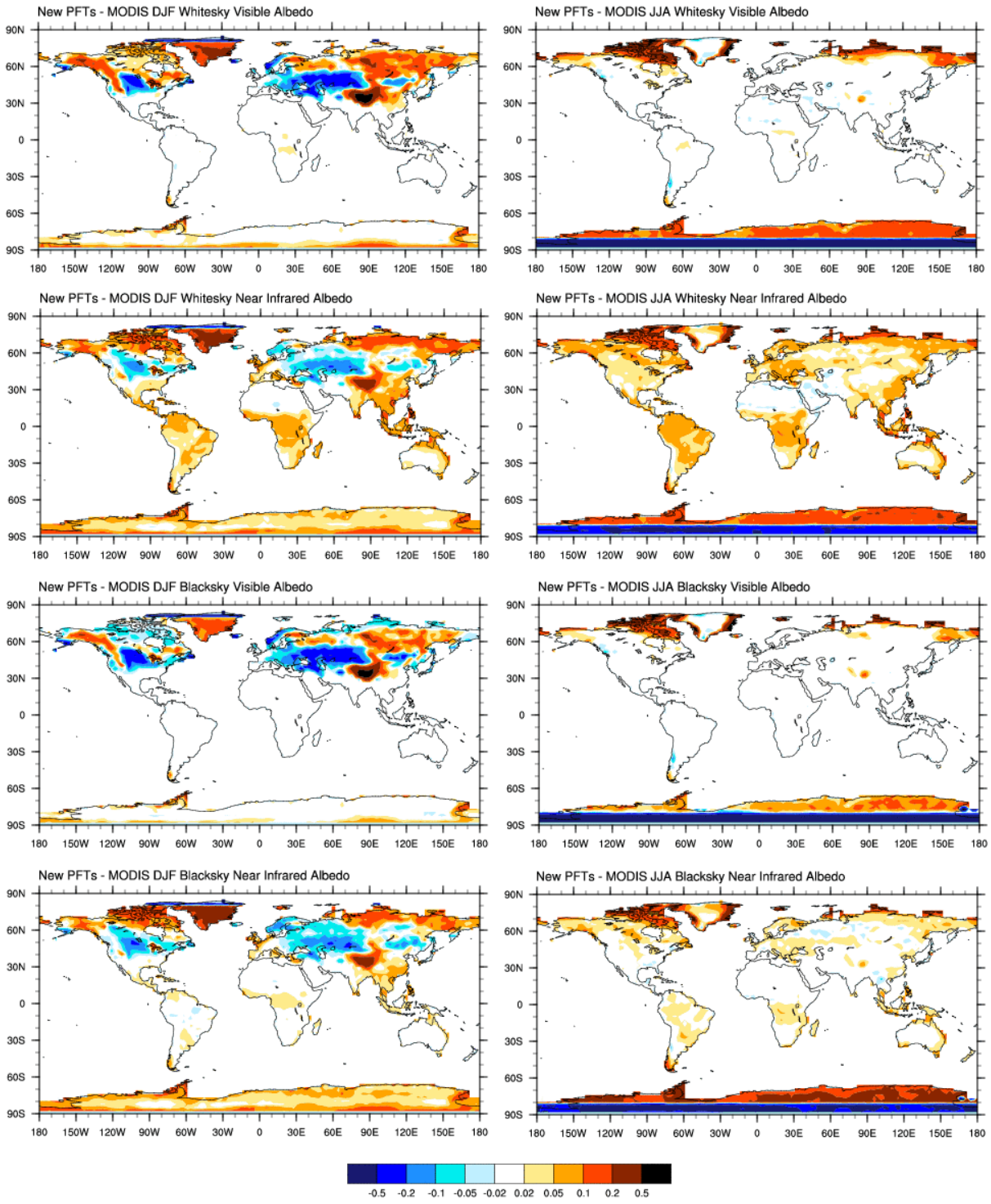

FIG. 5 Seasonal differences to MODIS of CLM Albedo at the T42 grid increment for New Parameters Experiment

In particular the difference in snow distribution between MODIS and the new parameter experiment (*figure 4*) appeared to make a large contribution to the albedo differences. In areas where the MODIS and model snow distributions were consistent, there also were albedo differences between the new parameters experiment and MODIS. In general these differences were smaller in the new parameters experiment than in the current parameters experiment (not shown), suggesting the albedo differences between the model and MODIS also were reduced in these areas with the denser vegetation canopies of the new parameters.

The impact of the higher albedo on the high JJA precipitation biases over the Saudi peninsula raises important questions as to the impact of snow affected albedo differences to the north of this region in Europe, Eurasia and the Tibetan plateau. The reduction in the cool JJA bias over the Sahel also was of interest as it was associated with an increase in surface albedo. The most probable cause of the warming over this region was the decrease in precipitation with subsequent impacts on evaporation and surface energy balances.

8. CONCLUSIONS

The new methods used to derive CLM PFT, LAI, SAI and radiation parameters from AVHRR and MODIS satellite data, significantly reduced the differences between the CLM and MODIS in snow free areas. In snow affected areas however, where the new parameters effectively removed differences in surface albedo due to soil and vegetation, the remaining albedo differences revealed that the snow impacts on albedo raised by *Oleson et al.*, (2003) were consistent in the model regardless of the vegetation and soil parameters. The snow albedo differences also were of larger magnitude than the vegetation and soil differences raising the question as to what impacts the snow albedo differences have on climate simulation in the CCSM. While the impacts on climate simulated in the CCSM with the new parameters were in general mixed, the reduction in the large JJA precipitation bias over the Saudi peninsula and the Sahel showed the importance of accurately representing surface radiation budgets and surface energy balances in the simulation of climate in the CCSM.

ACKNOWLEDGEMENTS

This research was made possible by a grant from the National Center for Atmospheric Research, which is sponsored by the National Science Foundation, for use the computing time for model experiments.

REFERENCES

Bonan, G.B., S. Levis, L. Kergoat, and K.W. Oleson, Landscapes as patches of plant functional types: An integrated concept for climate and ecosystem models, *Global Biogeochemical Cycles*, *16* (2), 1021-1051, 2002.

Defries, R.S., M.C. Hansen, J.R.G. Townshend, A.C. Janetos, and T.R. Loveland, A new global 1-km dataset of percentage tree cover derived from remote sensing, *Global Change Biology*, *6*, 247-254, 2000.

Myneni, R.B., R.R. Nemani, and S.W. Running, Estimation of Global Leaf Area Index and Absorbed Par Using Radiative Transfer Models, *IEEE Transactions on Geoscience and Remote Sensing*, *35* (6), 1380-1393, 1997.

Nemani, R., and S.W. Running, Implementation of a hierarchical global vegetation classification in ecosystem function models, *Journal of Vegetation Science*, *7*, 337-346, 1996.

Oleson, K.W., G.B. Bonan, C. Schaaf, F. Gao, Y. Jin, and A.H. Strahler, Assessment of global climate model land surface albedo using MODIS data, *Geophysical Research Letters*, *30* (8), 1443-1447, 2003.

Schaaf, C.B., F. Gao, A.H. Strahler, W. Lucht, X. Li, T. Tsang, N.C. Strugnell, X. Zhang, Y. Jin, and J.-P. Muller, First operational BRDF, albedo nadir reflectance products from MODIS, *Remote Sensing of Environment*, *83* (1-2), 135-148, 2002.

Sitch, S., B. Smith, I.C. Prentice, A. Arneth, A. Bondeau, W. Cramer, J.O. Kaplan, S. Levis, W. Lucht, M.T. Sykes, K. Thonicke, and S. Venevsky, Evaluation of ecosystem dynamics, plant geography and terrestrial carbon cycling in the LPJ dynamic global vegetation model, *Global Change Biology*, *9*, 161-185, 2003.

Still, C.J., J.A. Berry, G.J. Collatz, and R.S. DeFries, Global distribution of C3 and C4 vegetation: Carbon cycle implications, *Global Biogeochemical Cycles*, *17* (1), 1006-1019, 2003.

Tian, Y., R.E. Dickinson, L. Zhou, R. Myneni, M. Friedl, C. Schaaf, M. Carroll, and F. Gao, Land boundary conditions from MODIS data and consequences for the albedo of a climate model, *Geophysical Research Letters*, *31* (5), L05504, 2004a.

Tian, Y., R.E. Dickinson, L. Zhou, X. Zeng, Y.J. Dai, R.B. Myneni, Y. Knyazikhin, X. Zhang, M. Friedl, H. Yu, W. Wu, and M. Shaikh, Comparison of seasonal and spatial variations of leaf area index and fraction of absorbed photosynthetically active radiation from Moderate Resolution Imaging Spectroradiometer (MODIS) and Common Land Model, *Journal of Geophysical Research*, *109* (D0), 1103-1116, 2004b.

Willmott, C.J., and K. Matsuura, Terrestrial air temperature and precipitation: Monthly and annual climatologies (Version 2.0.1) [Available online at http://climate.geog.udel.edu/~climate/html_pages/download.html], 2000.

Zeng, X., M. Shaikh, Y. Dai, R.E. Dickinson, and R. Myneni, Coupling of the Common Land Model to the NCAR Community Climate Model, *Journal of Climate*, *15*, 1832-1854, 2002.